International Journal of Thermophysics, Vol. 20, No. 1, 1999

The Effects of Different Property Models in a Computational Fluid Dynamics Simulation of a Reciprocating Compressor[1]

A. P. Peskin[2]

Computational fluid dynamics was applied to model a simple reciprocating compressor using R134a (1,1,1,2-tetrafluoroethane) as the working fluid. The sensitivity of the compressor model to various property models was quantitatively assessed by calculating the work required to carry out several compression cycles. The ideal gas equation, a virial equation using only the second virial coefficient, and the Peng–Robinson equation were compared to a reference-quality Helmholtz energy equation of state. Significant errors, up to 12% in the density of the outflowing gas, can result from the use of the ideal gas model. The Peng–Robinson equation resulted in density errors up to 6.3%. The virial equation gave values closest to those calculated using the Helmholtz energy equation of state, with errors in density up to 4.7%. The results also show that an increase in accuracy in work and mass flow calculations achieved by using the Helmholtz energy equation of state is obtainable without an impractical increase in computation time.

KEY WORDS: compressors; computational fluid dynamics; moving boundaries; property models.

1. INTRODUCTION

Computational fluid dynamics (CFD) and associated rigorous modeling of heat- and mass transfer offer accurate representations of physical processes. These can provide sound approaches by which to quantitatively assess the

[1] Paper presented at the Thirteenth Symposium on Thermophysical Properties, June 22–27, 1997, Boulder, Colorado, U.S.A.

[2] Physical and Chemical Properties Division, National Institute of Standards and Technology, 325 Broadway, Boulder, Colorado 80303, U.S.A.

0195-928X/99/0100-0175$16.00/0

importance of accurate property models in process design. It is often more efficient to run a computer simulation to find out details about heat losses, effective valve sizes, and flow patterns than to build prototype systems. However, computer models are useful only if the information they provide is realistic. Many available commercial CFD software packages have built-in numerical simplifications, of which a typical user may not be aware. In particular, fluid properties are often treated as having constant values over large ranges of temperature and pressure, or are modeled using the ideal gas law for compressible flow. Adding different property models into our own CFD software allowed us to determine the quantitative improvement gained by using accurate property models. The movement and flow of gas through a simplified reciprocating compressor using four property models that vary both in accuracy and computational speed are described here.

2. EQUATIONS OF MOTION

The compressor for this study is a reciprocating compressor, with R134a (1,1,1,2-tetrafluoroethane as the working fluid). Each cycle of the compressor has four stages: intake, compression, exhaust, and expansion. The flow of gas in each stage is modeled using the following set of equations describing conservation of momentum and mass.

Momentum equation:

$$\rho\left(\frac{\partial \mathbf{u}}{\partial t}+\mathbf{u}\cdot\nabla\mathbf{u}\right)=-\nabla P+\mu\,\nabla^2\mathbf{u}+\rho\mathbf{g} \tag{1}$$

Continuity equation:

$$\frac{\partial \rho}{\partial t}+\rho\nabla\cdot\mathbf{u}+\mathbf{u}\cdot\nabla\rho=\mathbf{0} \tag{2}$$

Energy equation:

$$\rho C_{\mathrm{p}}\left(\frac{\partial T}{\partial t}+\mathbf{u}\cdot\nabla T\right)=k\,\nabla^2 T+\left(\frac{\partial P}{\partial t}+\mathbf{u}\cdot\nabla P\right) \tag{3}$$

where ρ is the density, μ the viscosity, C_{p} the heat capacity, and k the thermal conductivity. The last two terms of the energy equation account for the effects of expansion and compression [1, 2].

3. EQUATIONS OF STATE

Four equations of state are used in this paper for calculating density for the conservation equations above, and for calculating enthalpy for additional information on compressor work. The first equation,

$$\rho = \frac{RT}{P}; \qquad \Delta H^0 = \int C_p^0 \, dT \tag{4}$$

is the ideal gas law. Ideal gas heat capacities are computed using a polynomial correlation for the ideal gas heat capacity [3]. The same correlation for ideal gas heat capacity (C_p^0) is used in all of the enthalpy calculations that follow. Each has both an ideal gas term, as given above, and a real gas term that varies from model to model. All other fluid properties are assigned constant values, $\mu = 0.00012\ \mathrm{g \cdot cm^{-1} \cdot s^{-1}}$, $k = 0.0138\ \mathrm{W \cdot m^{-1} \cdot K^{-1}}$, which are values averaged over the temperature and pressure range used here.

The second model is a simple virial equation of state truncated at the second virial coefficient. The second virial coefficient is represented as a polynomial function of temperature [4]. Enthalpies are found using Ref. 5. The equations are

$$\frac{P}{RT\rho} = 1 + B(T)\,\rho \tag{5}$$

$$\Delta H = \int C_p^0 \, dT - \Delta H^* = \Delta H^0 - \Delta H^* \tag{6}$$

$$\frac{\Delta H^*}{RT} = \frac{P}{R}\left(\frac{dB}{dT} - \frac{B}{T}\right) \tag{7}$$

The Peng–Robinson equation is used as an example of a cubic equation of state [6]:

$$P = \frac{RT}{V-b} - \frac{a}{V^2 + 2bV - b^2} \tag{8}$$

$$b = \frac{0.07780 RT_c}{P_c} \tag{9}$$

$$a = \frac{0.45724 R^2 T_c^2}{P_c}\left[1 + f_w(1 - T_r^{1/2})^2\right] \tag{10}$$

$$\Delta H = \int C_p \, dT - \Delta H^* = \Delta H^0 - \Delta H^* \tag{11}$$

$$\Delta H^* = RT(Z-1) + \left(\frac{T(\partial a/\partial T) - a}{2\sqrt{2b}} \right) \ln \left(\frac{Z + 2.44B^*}{Z - 0.414B^*} \right) \tag{12}$$

$$Z = \frac{PV}{RT} \tag{13}$$

$$B^* = \frac{bP}{RT} \tag{14}$$

where T_c and P_c are the critical temperature and pressure, T_r is the reduced temperature, T/T_c, and f_w, is a function of the acentric factor and, for R-134a, is evaluated as the constant value 0.849878.

The last property model used here is an optimized Helmholtz energy equation of state, based on the reference-quality correlation of Tillner–Roth and Baehr [7], which is currently used in the NIST REFPROP database, Version 6 [8]. This Helmholtz energy formulation has been accepted as the international standard for the properties of R134a, and all other models used in this work are compared to this equation.

The different density models are compared on the basis of compressor work required per cycle. Work is defined as the difference between the net heat transfer (Q) and the change in enthalpy (H) during compression. The process is assumed here to be adiabatic ($Q = 0$), so that the total work requirements for each of the different models was calculated.

4. NUMERICAL MODEL

Each stage of the compression cycle has its own set of boundary conditions. During the intake stage, the piston moves to expand the compressor volume and causes low pressure gas to flow into the cylinder. The intake valve is then closed, and the gas is compressed. When the pressure of the cylinder reaches the condenser pressure, the exhaust valve is opened, releasing the high pressure gas. The exhaust valve is then closed, and the gas is again expanded. The intake valve is opened when the pressure in the cylinder reaches the pressure of the intake gas. A complete cycle describes a sinusoidal pattern of the position of the piston with time.

Temperature boundary conditions are needed to complete the numerical description for the energy equation used to solve for the distribution of temperatures across the cylinder. A time-dependent temperature constraint

was assigned for the gas along the top and bottom walls of the cylinder. Values changed with cycle time, ranging from 253 K, when the intake valve opens, to the maximum temperature of the condenser, when the exhaust valve closes, which varied between the models. Assuming constant entropy as the gas is compressed the maximum temperature is calculated from a fixed pressure of the condenser (1.01254 MPa) and the entropy of the saturated vapor at 253 K. Maximum temperatures for the different models are 311.18 K for the ideal gas model, 321.75 K for the virial models 320.19 K for the Peng–Robinson model, and 321.65 K for the Helmholtz energy model. These are the constrained temperatures along the top and bottom boundaries when the exhaust valve closes. The variation of the temperature during an entire cycle is shown for all four models in Fig. 1, which starts at the beginning of gas expansion. The temperature range for the entire cycle of the ideal gas model is 58.18 K, which is 15.3% smaller than the 68.65 K range found using the Helmholtz energy model. A lower temperature significantly effects the mass flow of gas during the exhaust stage, as is seen in the CFD study.

The geometric domain is a cross-sectional slice of a cylinder 5 cm in diameter and 5 cm high when maximally expanded. Only half of the cross-section need be modeled due to symmetry. The height of the cylinder varies from 5 to 0.1 cm during compression. Our original mesh contained 533

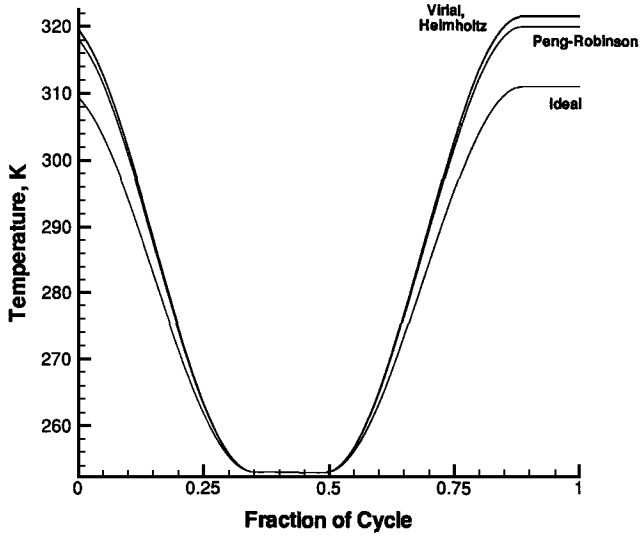

Fig. 1. Variation of temperature at a selected element over a complete compressor cycle.

nodes, a 20×6 array of "9-node" elements, which give quadratic approximations to the solutions of the global equations across the elements. The finite elements are constructed so that as they compress and expand, the ratio of lengths of adjacent sides is never higher than 8. Figure 2 shows the domain at two different cycle times, in both the expanded and compressed stages. When the mesh was refined to a 1159-node, a 30×9 array of elements, there was no significant change in the results. The 533-node mesh was used for all the simulations for the results presented here.

The elements compress or expand by moving nodes along parameterized lines. In this mesh, the lines are vertical and extend from the top of the cylinder to the bottom. Nodes along each line remain at constant relative distances from one another. Solutions were carried out using our current finite element software. For additional information about the software or the moving boundary method, see Peskin and Hardin [9].

At each time step, solutions are found for the temperatures, velocities, pressures, and corresponding densities of each element. The enthalpy is also calculated for each element, based on the temperature and density of the element. The overall enthalpy is the sum of the contributions of individual elements. The CFD study is necessary to find the variation of the enthalpy across the cylinder. The domain is then expanded or compressed as the

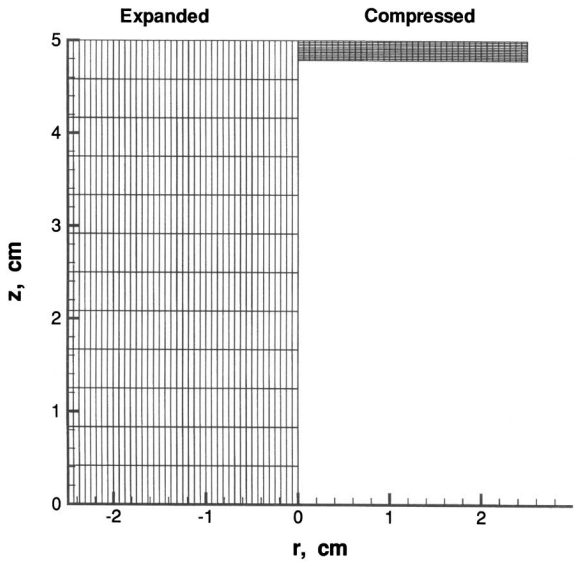

Fig. 2. A 553-node mesh at maximum expansion and compression.

piston moves, and enthalpy is calculated at each time step. The compressor is run at 1800 cycles per minute.

5. RESULTS

The CFD model of the compressor gives precise temperature and pressure contours across the cylinder, yielding quantitative information about density differences among the property models. Overall, the gas flow streamlines and the temperature and density contours followed similar patterns using the four different models, although the values of the properties varied from model to model. Temperatures inside the cylinder were highest in the center of the cylinder. There was significant variation in exit velocities. These velocities are a function of exhaust density and temperature, as outlined below.

Gas densities are directly related to the mass flow rate of the exhaust gas, and therefore critical to the design of the compressor. Figure 3 shows densities across the entire temperature-pressure range of the compressor for a single element selected from the center of the mesh. The differences between the models are seen in Fig. 4, which shows percentage density differences from densities calculated using the Helmholtz energy model for that element. The virial model comes closest to representing the reference

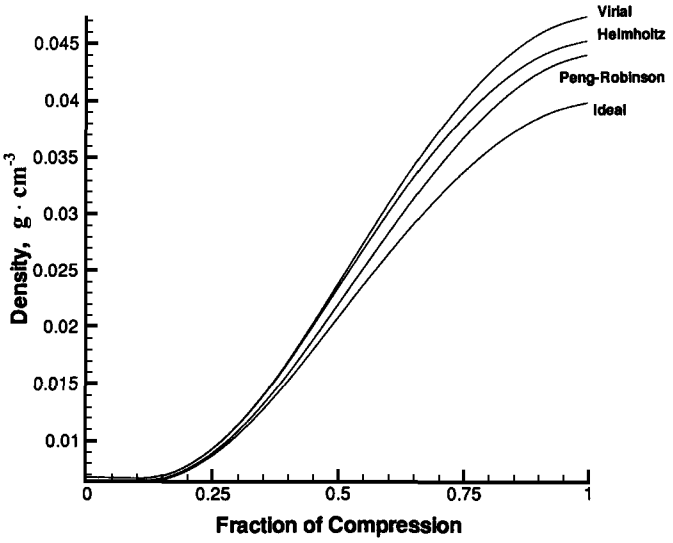

Fig. 3. Densities at a selected element over the T, P range of the compressor.

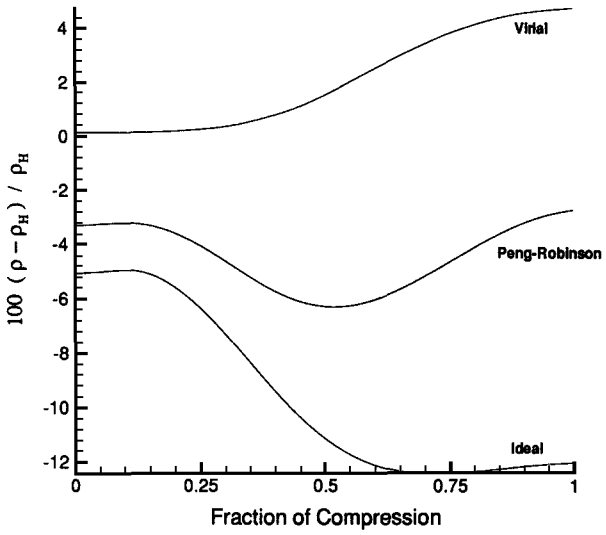

Fig. 4. Densities calculated with other models compared with the Helmholtz energy model.

densities, at least in the earlier compressor stages. It gives densities that steadily increase from 0.15% to 4.7% higher than densities calculated using the Helmholtz energy model. The Peng–Robinson densities are consistently lower than those calculated using the Helmholtz energy model, by approximately 3% in both the high and low pressure ranges. Densities diverge as much as 6.3% at midcycle from the reference values. The ideal gas law gives densities that are lower than the reference values by more than 12% at maximum compression. For comparison, a density calculated using the ideal gas law, but at 321 K and 1.01254 MPa, condenser conditions for the Helmholtz energy model, is 15% lower than the corresponding value calculated using the Helmholtz energy model.

Figure 5 shows the increase in the overall enthalpy of the compressor as a function of compression cycle using the four models, representing the work required to run the compressor. The virial equation of state most closely follows the Helmholtz energy model as shown in Fig. 6. This figure shows enthalpy differences from values calculated using the Helmholtz energy model. Figures 5 and 6 incorporate values from the entire cylinder, not just a single element. All three models have higher enthalpy difference values than the reference values. The shapes of the three difference curves follow a similar pattern, with the greatest differences at mid-compression. Values calculated from the virial equation stay within $1.2\ J \cdot g^{-1}$, varying 2 to 13% from values calculated using the Helmholtz energy model. The

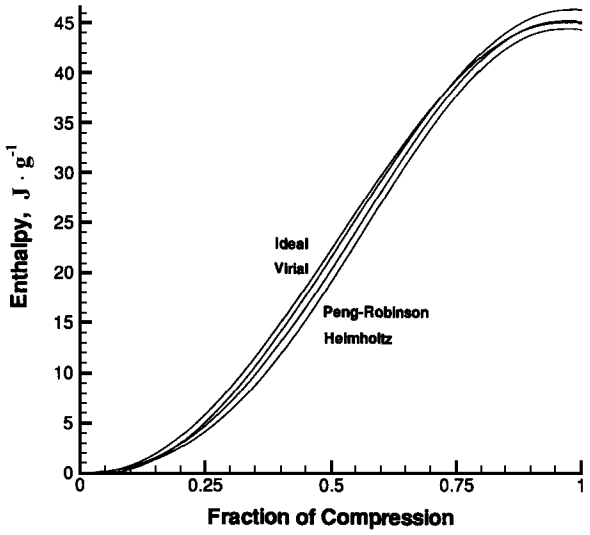

Fig. 5. Dependence of the system enthalpy on property model and stage of compression.

Peng–Robinson equation yields enthalpy values that diverge increasingly up to $3.3\,J \cdot g^{-1}$ at midcycle, which are 15 to 20% different from reference values. Errors drop to 2 to 3% toward the end of the cycle. The ideal gas enthalpies fall between the other two models at midcycle, and have larger errors than the other two models at the end of the cycle. Midcycle errors are 5 to 15%, and approximately 4% in the last third of the cycle. Differences decrease toward the end of compression due to the fact that enthalpies increase as a strong function of temperature. Since ideal gas enthalpies are greater than real gas enthalpies, this reduces the gap between the ideal gas and real gas models.

A constant value for the ideal-gas heat capacity C_p^0 is used in most commercial CFD software. This can also lead to appreciable error in design calculations. For comparison, a constant C_p^0 value was used in a simulation using the ideal gas law to calculate properties. The constant value was taken at 282 K, at the middle of the temperature range of the compressor. The resulting enthalpies are also shown in Fig. 6. The curve has the same shape as the curve for the ideal gas calculations using a variable C_p^0, but the errors are significantly (up to 30%) higher.

A series of timing tests were performed to analyze the effects, if any, of the improved property models on the computational time for simulating one complete cycle. All of the models except the Helmholtz energy model had virtually identical runtimes. Using the Helmholtz model resulted in an

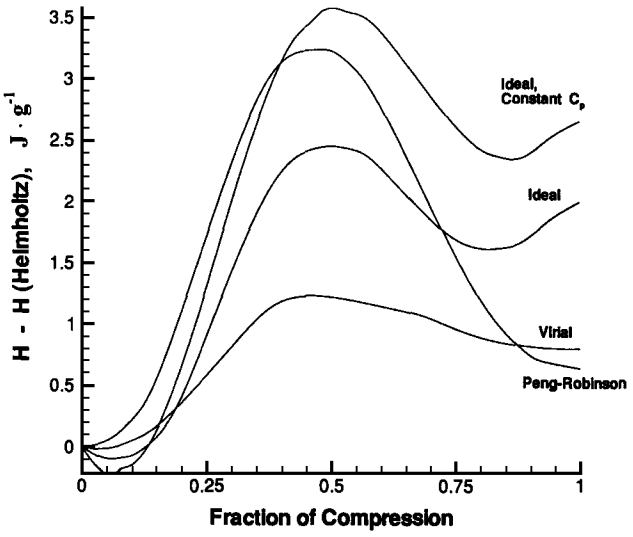

Fig. 6. Enthalpy calculated with other models compared with the Helmholtz energy model.

86% increase in time, 34 vs. 18.5 min. It is not an impractical increase considering the accuracy achieved in regions of high pressure.

The size of the geometric domain and the resulting global matrix of equations to be solved make a large difference to the percent increase in computation time using a complex property model. The larger the number of global equations, the greater the fraction of the total runtime spent solving the equations. A second set of timing tests was carried out with the refined, 1159-node mesh, comparing the Helmholtz energy model to the ideal gas model. The results showed an increase of only 60% computation time, approximately 57 min using the ideal gas model, versus 91 minutes using the Helmholtz energy model.

6. DISCUSSION AND CONCLUSIONS

The purposes of this work were to demonstrate the influence of accurate property models on simulation results and to examine the computational costs of the additional accuracy. The choice of an appropriate property model varies according to the particular CFD simulation, its temperature and pressure ranges, the size of the computational mesh, and the particular design information sought. A complex density model may not be necessary for every application, but it can make a large difference to applications in which the ideal gas model cannot accurately represent the

fluid property information. For the present example of a refrigeration compressor, the most complex model, the Helmholtz energy equation of state, resulted in a significant improvement in predicting densities and enthalpies inside the compressor. Using the CFD model, we can make quantitative measurements of this accuracy over the course of the simulation. Overall, the use of the virial equation produced errors of only a few percent. The pressures used in this simulation were within the range of validity of the virial equation. At higher pressures, errors approaching those using the ideal gas law would be expected for the virial equation. The Peng–Robinson equations gave higher errors, particularly at midcompression of the gas, where densities diverged as much as 6%, and enthalpy changes 5 to 15% from the reference values. The ideal gas law gave large differences in output temperatures, which somewhat masked significant differences from the Helmholtz model in work and mass flow.

REFERENCES

1. M. J. Assael, L. Karagiannidis, S. M. Richardson, and W. A. Wakeham, *Int. J. Thermophys.* **13**:223 (1992).
2. J. J. Healy, J. J. de Groot, and J. Kestin, *Physica* **82**:392 (1976).
3. B. A. Younglove and M. O. McLinden, *J. Phys. Chem. Ref. Data* **23**:731 (1994).
4. A. R. H. Goodwin and M. R. Moldover, *J. Chem. Phys.* **93**:2741 (1990).
5. J. M. Smith and H. C. Van Ness, *Introduction To Chemical Engineering Thermodynamics*, 3rd ed. (McGraw–Hill, New York, 1975).
6. D. Y. Peng and D. B. Robinson, *I.E.C. Fund.* **15**:59 (1976).
7. R. Tillner-Roth and H. D. Baehr, *J. Phys. Chem. Ref. Data* **23**:657 (1994).
8. M. O. McLinden and S. A. Klein, *Proc. 6th Int. Refrig. Conf.* (Purdue University, West Lafayette, IN, 1996), p. 409.
9. A. P. Peskin and G. R. Hardin, *Comput. Chem. Eng.* **20**:1043 (1996).